
Towards Efficient Vision-Language Tuning: More Information Density, More Generalizability

Tianxiang Hao^{1,2*}, Mengyao Lyu^{1,2*}, Hui Chen^{2†}, Sicheng Zhao²,
Xiaohan Ding³, Jungong Han⁴, Guiguang Ding^{1,2†}

¹School of Software, Tsinghua University ²BNRist

³Bytedance ⁴Computer Science Department, University of Sheffield
{beyondhtx, jichenhui2012, jungonghan77}@gmail.com
mengyao.lyu@outlook.com, {schzhao, dinggg}@tsinghua.edu.cn

Abstract

With the advancement of large pre-trained vision-language models, effectively transferring the knowledge embedded within these foundational models to downstream tasks has become a pivotal topic, particularly in data-scarce environments. Recently, parameter-efficient fine-tuning approaches, especially prompt tuning, have garnered considerable attention. To better understand the nature of prompt tuning, we propose the concept of “Information Density” (ID) to indicate whether a matrix strongly belongs to certain feature spaces rather than being evenly distributed across various feature spaces. We suppose a higher ID with strong bias across some feature spaces naturally leads to excellent robustness and stability. Our research, inspired by the observation that generalizability is closely linked to the information density of the prompt matrix, introduces the Dense Information Prompt (DIP). DIP aims to enhance information density to improve generalization. Furthermore, DIP significantly reduces the number of tunable parameters and the requisite storage space, making it particularly advantageous in resource-constrained settings. Comprehensive experiments substantiate the superiority of DIP. Notably, DIP surpasses the latest state-of-the-art methods by a substantial margin with an exceptionally small parameter count. Across a range of tasks spanning 11 datasets, DIP improves the average downstream accuracy of classic prompt tuning by up to 5.76% using merely 0.5K parameters.

1 Introduction

In recent years, vision-languages models [1, 2] have achieved tremendous success. Representative models like CLIP [1] are first pre-trained on a huge number of text-image pairs on the web to align textual and visual features, and then can be tuned and used for various downstream tasks.

However, traditional fine-tuning is not a good choice to adapt vision-language models. Simply fine-tuning all the parameters can easily cause the model to overfit because the huge number of parameters bring redundant non-essential information. The huge training and storage cost is also an intractable problem. In the context of our study, we introduce the concept of “information density”. Much like the rank of a matrix in linear algebra, which represents the maximum number of linearly independent rows or columns in the matrix, “information density” represents the maximum amount of essential and non-redundant information that the model can extract from the downstream task. Just as a matrix with a higher rank possesses more unique information, a model with high information

*Equal contribution

†Corresponding authors

density can acquire more essential and general information from the downstream task by fewer parameters, even with a smaller dataset. Our goal is increasing the information density and thus using the fewest but most essential parameters to finish generalization, without causing catastrophic forgetting or overfitting to the small dataset.

As the concept of information density can be functionally analogous to the rank of a matrix, we decided to use properties related to rank to quantify information density. Specifically, we take a full-rank matrix and decompose it using Singular Value Decomposition (SVD) to obtain a matrix of singular values, using the properties of these singular values to define and quantize information density. We found that this definition of information density is highly correlated with the model’s generalization performance (Spearman correlation coefficient > 0.9). Therefore, we propose DIP, aiming to enhance the model’s generalization ability by increasing information density. Additionally, due to the increased information carried by each parameter unit, our approach can significantly reduce the required number of parameters.

In Section 3, we will show our finding about the strong correlation between generalization capability and information density of the prompt matrix in Fig. 1. Inspired by such observation, we propose Dense Information Prompt (DIP) for effective and efficient adaptation, well adapting models under an extremely small number of parameters where nobody has explored before. There are several good advantages of DIP:

- **Efficiency and Effectiveness** To our knowledge, we are the first one to reach comparable or even better performance with state-of-the-art methods using such an extremely small number of parameters, *i.e.* 516.
- **Simplicity** Replacing the classic prompt by DIP just needs to modify several lines of code. No special loss nor extra module is introduced.
- **Robustness** DIP is relatively capable of anti-disturbance. As in Tab. 3, DIP could maximally reserve its knowledge from domain shift.
- **Plug and Play** For any classic model, DIP only replaces the prompts, enabling us to plug DIP into most of the existing methods fruitfully.

In summary, we conclude our contributions as follows:

- We propose a new concept “information density”, give its definition and well-quantize the concept. We further find the strong correlation between generalizability and information density in Fig. 1, and thus propose to use DIP to increase information density for better generalization capability.
- We propose a novel initialization method and integrate a lightweight regularization module to further improve the performance of Dense Information Prompt tuning without introducing any extra parameters and inference cost.
- We are the first to explore how to effectively adapt vision-language models using an extremely small number of parameters, *i.e.* 0.5K.
- We conduct extensive experiments and show the fantastic effectiveness and efficiency of DIP. In base-to-new generalization, domain generalization, cross-dataset transfer and few-shot learning settings, DIP consistently reaches very competitive results, surpassing many state-of-the-art tuning methods though we use fewer parameters.

2 Related Works

2.1 Vision-Language Models

Recently, large-scale vision-language models have shown very competitive performance in various tasks. Classic works [1, 2, 3, 4, 5] learn the multi-modal representation by a self-supervised manner on a large amount of image-text pairs. The representative work CLIP [1] is a milestone, which aligns the vision representation and language representation by contrastive learning and shows excellent performance. A well-trained vision-language model is a great treasure, which could largely facilitate the development of many fields. There have been successful applications of such strong models on few-shot recognition [6, 7], detection [8, 9, 10, 11] and segmentation [12, 13, 14, 15]. For video data, there are also works on video classification [16] and video understanding [17].

2.2 Prompt Tuning

Prompt tuning is one of the most popular methods to tune models in downstream tasks with excellent efficiency. Originating from natural language processing, prompts are first introduced as a fixed template [18], *e.g.* *a photo of a _*, which is hand-crafted and fixed. Later, a series of methods [19, 20, 21, 22, 23, 24] are proposed to make such prompts tunable and be optimized during adaptation. Prompt tuning could adaptively narrow the gap between pre-trained representations and downstream tasks, significantly facilitating the fine-tuning process. Representative prompt tuning methods would add tunable virtual tokens, *i.e.* prompts, along with the semantic tokens as inputs of the model. All of the tokens are processed together to get text embeddings first and then sent to the feature encoder. Witnessing the success of prompting language models, researchers design prompts [25, 26] for visual models in a similar way. In vision-language field, there are several explorations as well. Bahng *et al.* [27] adopts prompt tuning merely on the image encoder. CoOp [7] uses tunable text prompts to replace the fixed template in CLIP [1]. CoCoOp [6] utilizes image feature to instruct the optimization of the tunable text prompts in CoOp. [28, 29] simultaneously optimize image and text prompts and establish extra connections between different modals. [30, 31, 32, 33, 34] integrate strong regularization modules or losses into prompt tuning to diminish the overfitting and catastrophic forgetting problem. For better downstream accuracy, researchers design more and more complicated methods, accompanied by inefficiency. To solve the problem, we propose Dense Information Prompt (DIP) to take the place of classic prompts, which can largely decrease the number of tunable parameters and further enhance the model’s generalization ability. Notice that though becoming more complex, existing methods are still refined on a common fundamental basis, *i.e.* prompt tuning. Such a common basis guarantees that DIP could be easily and smoothly integrated into most of the off-the-shelf methods besides individually applied. Besides prompt-based methods, there are also many other works to acquire storage efficiency [35, 36, 37, 38, 26, 39], inference efficiency [40, 41, 42, 43, 44, 45, 46, 47, 48] and data efficiency [49, 50] during downstream tuning.

3 Relationship between Information Density and Generalizability

In this section, we will start from reviewing a classic prompt tuning pipeline CoOp [7] on CLIP in Section 3.1, and propose a new concept “Information Density” and analyze its relationship with generalizability in Section 3.2.

3.1 A Review of Prompt Tuning for CLIP

CLIP consists of a text encoder \mathcal{L} and an image encoder \mathcal{V} . Typically, \mathcal{L} is a language transformer, while \mathcal{V} can be a convolutional neural network or a vision transformer. In this paper, we follows [7, 6] to use a ViT-B/16 [51] as the image encoder \mathcal{V} unless specifically mentioned. We start by making a review of how to prompt a CLIP for prediction in the following paragraphs.

Text Encoder Suppose there are M layers in the text encoder. For k -th layer \mathcal{L}_k , the inputs are a series of prompt tokens P_{k-1}^l and a $[CLS]$ token c_{k-1}^l , and the outputs are P_k^l and c_k^l . The inputs of the first layer P_0^l and c_0^l are exactly the word embeddings of the prompts along with the label, *e.g.* “A photo of a $[CLS]$ ” or just some randomly initialized vectors. Formally, we have $P_k^l \in \mathbb{R}^{n^l \times d^l}$ and $c_k^l \in \mathbb{R}^{d^l}$, where n^l denotes the text prompts’ length and d^l denotes the dimension of word embedding. $\forall 1 \leq k \leq M$, we have $[P_k^l, c_k^l] = \mathcal{L}_k([P_{k-1}^l, c_{k-1}^l])$.

The output feature of the text encoder $f^l \in \mathbb{R}^{d^v}$, where d^v is the dimension of the visual feature space, is generated by projecting the $[CLS]$ token of the last layer to the visual space by a linear transformation, *i.e.* $f^l = \text{Proj}(c_M^l)$.

Image Encoder Suppose there are N layers in the image encoder. For k -th layer \mathcal{V}_k , the inputs are image patch tokens I_{k-1} , a classification token c_{k-1}^v and prompt tokens P_{k-1}^v , and the outputs are I_k , c_k^v and P_k^v . The inputs of the first layer I_0 and c_0^v are exactly the patch embeddings of the image and pre-trained class token. P_0^v is randomly initialized in general. Formally, we have $I_k \in \mathbb{R}^{p \times d^v}$, $c_k^v \in \mathbb{R}^{d^v}$ and $P_k^v \in \mathbb{R}^{n^v \times d^v}$, where p denotes the number of image patches and d^v denotes the dimension of visual embedding. $\forall 1 \leq k \leq N$, $[P_k^v, c_k^v, I_k] = \mathcal{V}_k([P_{k-1}^v, c_{k-1}^v, I_{k-1}])$. The output feature of the image encoder is $f^v = c_N^v$.

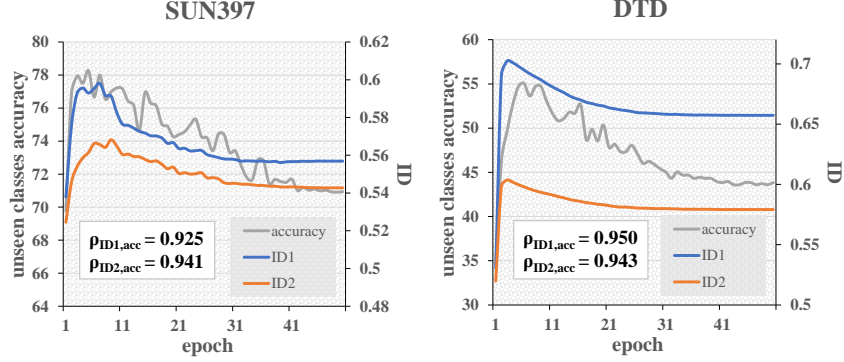


Figure 1: Relationship between generalizability represented by the test accuracy on unseen classes during training and Information Density (ID). When generalizability increases, ID also increases. The Spearman correlation coefficient ρ between generalizability and ID1/ID2 is very high, *i.e.* ≥ 0.9 .

Prediction CLIP can be used for image classification. Suppose there are C classes, and $\{f_c^l\}_{c=1}^C$ are the corresponding text features. Label y 's probability is $p(y|f^v) = \frac{\exp(\text{sim}(f^v, f_y^l)/\tau)}{\sum_{c=1}^C \exp(\text{sim}(f^v, f_c^l)/\tau)}$ where $\text{sim}(\cdot, \cdot)$ denotes cosine similarity function and τ is temperature. The final prediction is $\hat{z} = \arg \max_{1 \leq y \leq C} (p(y|f^v))$.

It is worth noting that some researchers adopt a deeper manner [25, 28] to organize the prompts. They directly add and tune the prompt in each layer in the feature encoder, instead of inheriting the output prompt calculated by the last encoder, *i.e.* a forward pass becomes $[-, c_k^l] = \mathcal{L}_k([P_{k-1}^l, c_{k-1}^l])$ and $[-, c_k^v, I_k] = \mathcal{V}_k([P_{k-1}^v, c_{k-1}^v, I_{k-1}])$. Each P^l/P^v contains tunable parameters.

3.2 Information Density in Prompt Tuning

Here, we first provide precise definitions for ‘‘information density’’ to clearly convey our motivations. For typical parameter matrix like prompts $P \in \mathbb{R}^{n \times d}$ (assume $n < d$), we can always rewrite such matrix into a combination of several orthogonal bases with different weights by singular value decomposition (SVD). Formally, $P = U\Sigma V^T = \sum_{i=1}^d \sigma_i u_i v_i^T$. Each $u_i v_i^T$ can span a unique feature space, and P is a linear combination of these features. Typically, $\{\sigma_i\}_{i=1}^n$ are arranged in descending order.

To help readers better understand the concept of information density, let’s draw an analogy using images from nature. A real image always has one or a few very prominent features and almost never contains an even mix of various odd features. In an extreme case, if an image truly exhibits isotropic characteristics, it would simply mean that its content is almost entirely noise and lacks clear meaning. Reflecting this back to the matrix decomposition we discussed earlier, a good image tends to have several significantly larger singular values. The features of the image can largely be expressed by the feature space behind these prominent singular values. Therefore, from the matrix decomposition expression, the differences among the singular values $\{\sigma_i\}_{i=1}^n$ are significant, indicating that the information is concentrated in a few feature spaces. In other words, the information density is higher. Thus, to quantize such property, we define k -th order ‘‘Information Density (ID)’’ as follows: $ID_k = \frac{\sum_{i=1}^k \sigma_i}{\sum_{i=1}^n \sigma_i}$. In other words, ID_k is the proportion of the largest k singular values among all the singular values. Greater information density represents more robust and stable intrinsic features, meaning they are less likely to be affected by external disturbances and have stronger anti-interference capabilities.

Returning to our initial discussion, a core contribution of this paper is the hypothesis and verification that the parameter matrices, like prompts, follow the same ID-related laws during fine-tuning in downstream CLIP models. As is well-known, in transfer learning, the transfer of knowledge in a model depends on the updating of parameters. For CLIP models, the optimal solution is prompt tuning [7, 6, 28, 52]. We first hypothesize that the information density of the prompt matrix also represents its robustness and the strength of its intrinsic features. Therefore, greater information density should theoretically result in better generalizability throughout the prompt tuning process.

Table 1: A quick check for different implementations of DIP.

| | base | new | H |
|---------|-------|-------|--------------|
| w/o any | 82.69 | 63.22 | 71.66 |
| Alg. 1 | 81.21 | 67.58 | 73.77 |
| Alg. 2 | 80.39 | 69.85 | 74.75 |
| Alg. 3 | 79.91 | 71.48 | 75.46 |

To verify this hypothesis, we conducted an experiment using a classic method, CoOp [7]. During training, we masked half of the classes, using data from only the other half for training, and performed singular value decomposition on the prompt matrices during the process. As shown in Fig. 1, for better visualization, ID1 is scaled up to 2x to be put under the same right axis with ID2. Unseen classes accuracy is improved in the first few iterations, but it starts dropping later, indicating overfitting and catastrophic forgetting. Importantly, the fluctuation trend of unseen classes accuracy is highly consistent with ID. We compute the Spearman correlation coefficient between unseen classes accuracy and ID1/ID2 in Fig. 1. Clearly, the first-order and second-order information densities of CoOp on the SUN397 [53] and DTD [54] datasets exhibit a very strong correlation with the accuracy on unseen classes (*i.e.*, generalizability), with Spearman correlation coefficients greater than 0.9. This demonstrates that our hypothesis is correct.

In the following Section 4, we will show how we can leverage such correlation between generalizability and ID to boost CLIP’s downstream performance.

4 Methodology

4.1 Dense Information Prompt

4.1.1 Algorithms for increasing information density

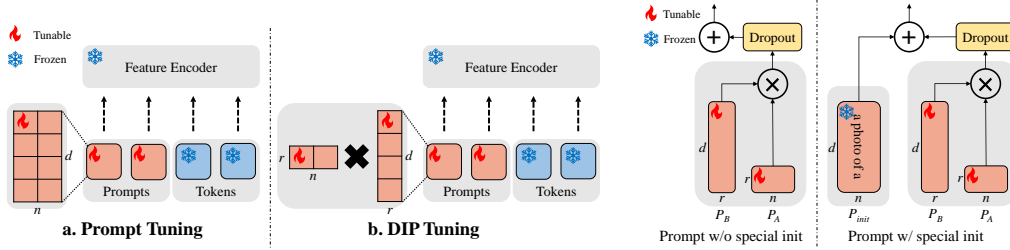
In this part, we aim to find an effective algorithm to increase information density to enhance CLIP’s downstream generalization performance. Motivated by the observation in Section 3, we propose three optional algorithms.

Alg. 1: Do SVD and directly optimize information density as an training objective. Specifically, we add corresponding expression to the loss item after decomposing prompt matrix by SVD. Suppose the original cross entropy loss is \mathcal{L}_{CE} and we want to maximize ID_k ($1 \leq k \leq n$), the current loss is $\mathcal{L} = \mathcal{L}_{CE} - \lambda ID_k$, where λ is a positive hyper-parameter.

Alg. 2: Do SVD and apply order-related penalty on the singular values. Specifically, we add regularization term to our optimization objective. Suppose the original cross entropy loss is \mathcal{L}_{CE} and we want to maximize ID_k ($1 \leq k \leq n$), the current loss is $\mathcal{L} = \mathcal{L}_{CE} + \lambda \sum_{i=n-k+1}^n i \|\sigma_i\|$.

Alg. 3: Approximate the original matrix by the product of two small matrices. Formally, given a typical prompt matrix $P \in \mathbb{R}^{n \times d}$, we take inspiration from LoRA [37] to create two low-dimensional matrices and use their product as an approximated equivalent prompt. Suppose we want to maximize ID_r ($1 \leq r \leq n$), we first randomly initialize $P_A \in \mathbb{R}^{n \times r}$ and $P_B \in \mathbb{R}^{r \times d}$. The low-rank approximated prompt $P_{lr} = P_A P_B$ is with the same shape with P , and thus can participate in the training.

We do a quick verification on several datasets used in the base-to-new generalization setting and show the results in Tab. 1. Clearly, from Alg. 1 to Alg. 3, the intensity of constraint is becoming stronger, resulting in more accuracy loss on base classes while enjoying more accuracy gain on new classes. In addition to the good performance, Alg. 3 has another advantages: it’s quite simple and easy to implement with faster training speed. Therefore, we choose Alg. 3 to implement our DIP. However, unlike LoRA who merely uses a similar low-rank product as a supplementary addition for the output of main branch, Alg. 3 directly outputs the product for usage, leading to some unique difficulties and challenges. We will show the problems behind such approximation and our solutions in the next sections.



(a) Comparison between DIP Tuning and Prompt Tuning. (b) DIP enjoys special initialization. Figure 2: To switch from classic prompt tuning and to DIP tuning, just replace the ordinary prompts with DIPs. DIP introduces two small parameter matrices in shape $[n, r]$ and $[r, d]$ separately, and uses their product as an equivalent prompt in shape $[n, d]$. For the prompts with special initialization, e.g. a hand-crafted template “a photo of a” for the text prompts, we introduce a concurrent full-rank prompt branch along with the proposed low-rank prompts. By turning off the gradient of the newly added branch, we start training from a promising initial point, and the total number of tunable parameters or stored parameters will not increase as well. The Dropout layer could effectively regularize the update of low-rank prompts and alleviate overfitting and catastrophic forgetting. Dropout is a lightweight non-parametric layer and turns out to be an Identity layer in inference, resulting in negligible cost.

4.1.2 Special Initialization

In the field of tuning vision-language models, existing works have confirmed that the initialization method of prompts is quite important. For example, [6, 7] adopt a hand-crafted template as the initial point of the text prompts, and [29] copies the parameters in the text or image class token to initialize the prompts of the corresponding branch. If we just do a random initialization, the overall performance of such existing methods would drop severely. See Section 5.2 for more details. In other words, it would be helpful if we could take advantage of a good initial point.

The problem lies in the fact that artificially designed initialization P_{init} is almost certain to be full rank, i.e. $\text{rank}(P_{init}) = \min(n, d)$, and our current low-rank prompt $P_{lr} = P_A P_B$ could only express the matrices whose rank is less or equal than r . Since $r < \min(n, d)$, it is impossible to directly initialize P_A and P_B by a given P_{init} .

To solve such a problem, we add a concurrent branch of full-rank prompts $P_{fr} \in \mathbb{R}^{n \times d}$ along with the proposed low-rank prompts as shown in Fig. 2b. Naturally, $P_{fr} = P_{init}$. And we randomly sample P_A/P_B from a Gaussian distribution in which $\mu = 0$ and $\sigma \rightarrow 0$. A small σ here could avoid constant initialization and enrich the update paths. Notably, P_{fr} is kept frozen during the whole adaptation, and thus it would not increase the number of tunable or stored parameters.

4.1.3 Regularization

As discussed in Section 2, existing works have shown that proper regularization would significantly improve the generalization ability. Therefore, to alleviate overfitting and catastrophic forgetting, we put a Dropout layer with drop ratio p after the low-rank branch as displayed in Fig. 2b.

Therefore, the input prompt of the feature encoder is $P = P_{fr} + \text{Dropout}(P_{lr}, p)$. Finally, we have $P = P_{init} + \text{Dropout}(P_A P_B, p)$.

4.2 Efficiency Analysis

The whole adaptation process of a pre-trained vision-language model can be divided into three parts: training, storage and inference. In this subsection, we will analyze the efficiency of DIP in each part separately.

Training In the training phase, the number of tunable parameters in total is $r(n + d)$. Compared with classic prompt tuning which has nd tunable parameters, we can largely reduce the trainable parameters by choosing a small r satisfying $r \ll \min(n, d)$. Such reduction could help us train the model faster and use less memory during training than those delicate-designed methods with massive complicated structures and update rules.

Storage After training, we just store P_A and P_B onto the disk for every downstream task. Similar to the training period, the number of stored parameters is $r(n + d)$. In contrast, classic prompt tuning

Table 2: Comparisons with latest methods in base-to-new generalization. H: harmonic mean [55]. In the lightweight methods, DIP+CoOp outperforms all the other competitors on new and harmonic mean accuracy. While in the heavy methods, DIP+MaPLe surpasses MaPLe [28] by a clear margin, and is strongest on base, new and harmonic mean accuracy, even with around only $\frac{1}{5}$ parameters compared with MaPLe.

| Method | #params | Base | New | H |
|--------------------|---------|--------------|--------------|--------------|
| Lightweight | | | | |
| CLIP [1] | 0K | 69.34 | 74.22 | 71.70 |
| CoOp [7] | 2.1K | 82.69 | 63.22 | 71.66 |
| CoCoOp [6] | 35.4K | 80.47 | 71.69 | 75.83 |
| Adapter [56] | 525.5K | 82.62 | 70.97 | 76.35 |
| LoRA [37] | 129.0K | 84.30 | 67.33 | 74.86 |
| ProGrad [52] | 8.2K | 82.79 | 68.55 | 75.00 |
| DIP+CoOp | 0.5K | 80.32 | 74.73 | 77.42 |
| Heavy | | | | |
| MaPLe [28] | 3548K | 82.28 | 75.14 | 78.55 |
| DIP+MaPLe | 741.9K | 83.17 | 75.43 | 79.11 |

Table 3: Comparisons with latest methods in domain generalization after tuned on ImageNet. DIP+CoOp shows excellent robustness when dealing with domain shift.

| #params | IN-V2 | IN-Sketch | IN-Adversarial | IN-Rendition | Average | |
|----------|--------|--------------|----------------|--------------|--------------|--------------|
| CLIP | 0K | 60.83 | 46.15 | 47.77 | 73.96 | 57.18 |
| CoOp | 2.1K | 64.20 | 47.99 | 49.71 | 75.21 | 59.28 |
| CoCoOp | 35.4K | 64.07 | 48.75 | 50.63 | 76.18 | 59.91 |
| Adapter | 525.5K | 62.53 | 47.67 | 49.17 | 75.42 | 58.70 |
| LoRA | 129.0K | 62.37 | 42.43 | 38.40 | 68.97 | 53.04 |
| ProGrad | 8.2K | 64.73 | 47.61 | 49.39 | 74.58 | 59.07 |
| DIP+CoOp | 0.5K | 63.95 | 49.07 | 50.97 | 77.19 | 60.30 |

stores a much larger set of nd parameters. As a result, we can save a fairly large amount of storage space when there are lots of tasks to be adapted.

Inference Before inference, we first load P_{init} , P_A and P_B from disk to memory. Noticing that Dropout is exactly an identity layer in the inference mode, we could pre-calculate the equivalent P by $P = P_{init} + P_A P_B$ and just keep P in the memory. For inference, we directly use P as the input prompts, and thus the inference cost is the same as classic prompt tuning. Some existing methods add complex bridges between the isolated parameters to earn extra improvements, *e.g.* CoCoOp [6]. There ain’t no such thing as a free lunch. They would face slower speed and huge memory occupation in inference time.

5 Experiments

To verify the effectiveness of the proposed method, we evaluate our method and make comparisons with the latest state-of-the-art methods in terms of the following settings in a wide range: base-to-new generalization, domain generalization, cross-dataset transfer and few-shot learning.

For more experimental details, please refer to the Appendix.

5.1 Main Results

5.1.1 Base-to-new Generalization

The average results over 11 datasets are shown in Tab. 2. For complete results, please refer to the Appendix. Overall, DIP shows the strongest performance, and the superiority mainly relies on the improvement of new classes. In other words, DIP largely improves the generalization ability of CLIP. In particular, compared with our direct baseline CoOp, DIP gets 10.95% accuracy gain on the new classes and 2.83% accuracy drop on the base classes. By adding DIP to the prompts as well as the linear layers of MaPLe, we earn an excellent **0.56%** performance gain while reducing its parameters to $0.2\times$ of the original parameters. Notably, compared with the latest lightweight method ProGrad, even if DIP only uses $<20x$ of its parameters, DIP still outperforms it by a clear margin, which clearly demonstrates the efficiency and effectiveness.

Table 4: Results in the cross-dataset transfer setting. DIP+CoOp gives the highest accuracy on 6 of 10 datasets, and slightly outperforms CoCoOp on average. Such result well demonstrates that DIP could maximally extract general and data-agnostic knowledge from given images.

| | # params | Caltech101 | Pets | Cars | Flowers | Food101 | Aircraft | Sun397 | DTD | EuroSAT | UCF101 | Average |
|----------|----------|--------------|--------------|--------------|--------------|--------------|--------------|--------------|--------------|--------------|--------------|--------------|
| CoOp | 2.1K | 93.70 | 89.14 | 64.51 | 68.71 | 85.30 | 18.47 | 64.15 | 41.92 | 46.39 | 66.55 | 63.88 |
| CoCoOp | 35.4K | 94.43 | 90.14 | 65.32 | 71.88 | 86.06 | 22.94 | 67.36 | 45.73 | 45.37 | 68.21 | 65.74 |
| Adapter | 525.5K | 93.43 | 88.87 | 64.40 | 70.27 | 85.63 | 24.67 | 65.80 | 44.90 | 47.70 | 66.00 | 65.17 |
| DIP+CoOp | 0.5K | 94.20 | 90.50 | 67.17 | 71.27 | 86.07 | 23.83 | 67.60 | 46.73 | 42.10 | 68.93 | 65.84 |

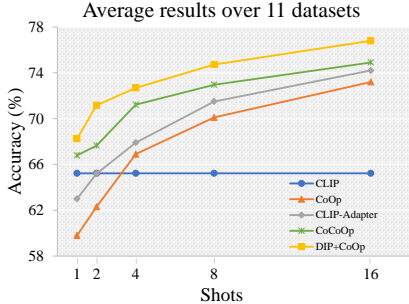


Figure 3: Few-shot learning Results.

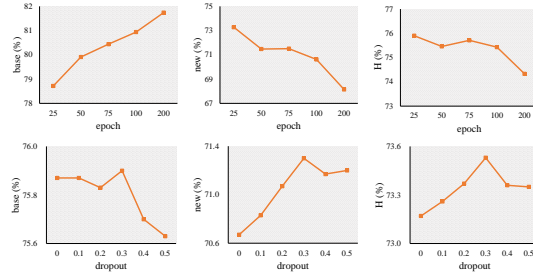


Figure 4: Top: Effect of training epochs. Bottom: Effect of dropout ratios.

5.1.2 Domain Generalization

Then we follow CoCoOp [6] to use ImageNet, ImageNet-A, ImageNet-R, ImageNet-v2, and ImageNet-S to run domain generalization experiments to verify the robustness of DIP (DIP = DIP + CoOp, and the same applies thereafter, unless otherwise specified.). Shown in Tab. 3, on target datasets, DIP leads to better average accuracy compared with the latest methods, largely outperforming CLIP, CoOp, CLIP-Adapter and ProGrad with much fewer parameters.

5.1.3 Cross-dataset Transfer

Finally, we follow CoCoOp [6] to conduct cross-dataset transfer evaluation. Results are shown in Tab. 4. Concentrating too much on the current dataset will absolutely cause overfitting and catastrophic forgetting problems, and finally lead to a severe drop in the performance on those unseen datasets. In this setting, DIP wins on 6 of 10 datasets and its average accuracy is also slightly better than the best competitor CoCoOp. Such result well demonstrates that DIP could maximally extract general and data-agnostic knowledge from given images compared with other prompt-based methods. Considering the huge difference in the parameter numbers, we could summarize that DIP is still the better choice.

5.1.4 Few-shot Learning

In this paragraph, we will show the experiment results of DIP in the few-shot learning setting. This setting is originated from CoOp. Seen from Fig. 3, DIP consistently outperforms zero-shot CLIP, CoOp, and CLIP-Adapter across all the shot numbers. Such results demonstrate the superiority of DIP in adaptation ability when there are few samples in downstream tasks.

Overall, in base-to-new generalization, domain generalization, cross-dataset transfer and few-shot learning, DIP can be fruitfully integrated into existing methods and consistently reaches state-of-the-art performance while enjoying extremely high parameter efficiency.

5.2 Analysis

5.2.1 Ablation study

We first show the impact of components of DIP step by step.

Table 5: Ablation study on base-to-new generalization setting

| | Decomposition | Full-rank init | Dropout | #params | base | new | H |
|----------|---------------|----------------|---------|---------|--------------|--------------|--------------|
| CoOp | - | - | - | 2.1K | 82.69 | 63.22 | 71.66 |
| DIP+CoOp | ✓ | - | - | 0.5K | 79.91 | 71.48 | 75.46 |
| | ✓ | ✓ | - | 0.5K | 79.42 | 73.21 | 76.19 |
| | ✓ | ✓ | ✓ | 0.5K | 79.70 | 73.59 | 76.53 |

Table 6: Results on ResNet-50 encoded CLIP. Table 7: Effect of DIP’s rank on ImageNet.

| | #params | base | new | H |
|----------|---------|--------------|--------------|--------------|
| CoOp | 2.1K | 77.16 | 61.01 | 68.14 |
| ProGrad | 8.2K | 73.29 | 65.96 | 69.06 |
| DIP+CoOp | 0.5K | 75.22 | 64.98 | 69.73 |

| rank | #params | base | new | H |
|------|---------|--------------|--------------|--------------|
| 1 | 0.5K | 75.87 | 70.67 | 73.17 |
| 2 | 1.0K | 76.03 | 70.13 | 72.96 |
| 3 | 1.5K | 76.20 | 70.40 | 73.19 |

We start from transforming the text encoder. We first replace the tunable prompt tokens with our decomposed small prompt matrices, denoted as “Decomposition”, for the CoOp method. After such replacement, the average Harmonic accuracy over 11 datasets directly improved from 71.66% to 75.46%. The accuracy on the base classes decreases by 2.78% and on the new classes increases by 8.26%. Although the adaptation ability slightly drops, the generalization ability raises quite a lot. This phenomenon proves that our low-rank design is fairly beneficial for the model’s generalization ability once again. Then we integrate the special full-rank initialization into CoOp. The harmonic mean accuracy improves by 1.27%. Finally, we add a lightweight regularization layer, Dropout. It helps us alleviate overfitting and catastrophic forgetting, resulting in further improvement.

5.2.2 Additional experimental results

Effect of different training epochs In this paragraph, we investigate that how the total training epoch could influence the adaptation result. Shown in Fig. 4, we run experiments for the given epochs separately. As the training epoch increases, the accuracy on base classes continues decreasing while the accuracy on new classes continues increasing. It is reasonable because as the training continues, the model has a higher risk of forgetting its original knowledge and overfitting.

Effect of different dropout ratios In this paragraph, we will show the influence of different dropout ratios in DIP on ImageNet. Seen from Fig. 4, as the dropout ratio increases, the base accuracy starts decreasing while the new accuracy starts increasing mostly. The harmonic mean first increases and then decreases. Dropout is a kind of regularization, only proper regularization can help avoid overfitting and catastrophic forgetting.

CLIP with convolutional image encoder In this paragraph, we show the results of DIP on CLIP with convolutional image encoder ResNet-50 [57], rather than the default ViT-B/16 [51]. Seen from Tab. 6, compared with baseline CoOp, DIP still largely improves the new accuracy and the harmonic mean accuracy over 11 datasets, while the base accuracy slightly drops. Compared with the latest method ProGrad, DIP shows clear superiority on base accuracy and the harmonic mean accuracy.

Effect of different ranks In this paragraph, we will show the influence of different ranks in DIP. Seen from Tab. 7, roughly, a larger rank brings more parameters, higher base accuracy, and lower new accuracy. As a result, increasing rank is not necessarily able to improve the average accuracy.

Results for using DIP on the image prompts There are several works [25, 28] indicating the effectiveness of the image prompts. Therefore, in this subsection, we will explore the results of applying DIP to image prompts. Seen from Tab. 8, using DIP on the image side also reaches high accuracy. However, the base, new, and average accuracy of image DIP is not as good as those of text DIP. Such experiment result tells us to use DIP on the text side instead of the image side when we aim to reach high accuracy with extremely few parameters.

Table 8: Results of adding DIP to image prompts on ImageNet.

| | #params | base | new | H |
|-----------|---------|--------------|--------------|--------------|
| Text DIP | 0.5K | 75.87 | 70.67 | 73.17 |
| Image DIP | 0.5K | 74.57 | 69.40 | 71.89 |

6 Conclusion

With the development of huge vision-language models, how to effectively and efficiently adapt such huge models to downstream tasks becomes a challenging problem. Much effort has been made to leverage the potential of prompt tuning in adapting vision-language models. However, existing methods suffer from inefficiency. To reach extremely efficient generalization, we propose Dense Information Prompt (DIP) based on the observation about the strong correlation between prompt rank and generalizability. Moreover, we propose a novel initialization method and a lightweight regularization module to further improve the low-rank design without adding any extra inference cost. We are the first to explore how to effectively adapt vision-language models using an extremely small number of parameters, *i.e.* 0.5K. Besides efficiency and effectiveness, DIP has many valuable advantages such as simplicity and robustness. Extensive experiments and analyses show the superiority of DIP sufficiently.

References

- [1] Alec Radford, Jong Wook Kim, Chris Hallacy, Aditya Ramesh, Gabriel Goh, Sandhini Agarwal, Girish Sastry, Amanda Askell, Pamela Mishkin, Jack Clark, et al. Learning transferable visual models from natural language supervision. In *International Conference on Machine Learning*, pages 8748–8763. PMLR, 2021.
- [2] Chao Jia, Yinfei Yang, Ye Xia, Yi-Ting Chen, Zarana Parekh, Hieu Pham, Quoc Le, Yun-Hsuan Sung, Zhen Li, and Tom Duerig. Scaling up visual and vision-language representation learning with noisy text supervision. In *International Conference on Machine Learning*, pages 4904–4916. PMLR, 2021.
- [3] Xiaohua Zhai, Xiao Wang, Basil Mustafa, Andreas Steiner, Daniel Keysers, Alexander Kolesnikov, and Lucas Beyer. Lit: Zero-shot transfer with locked-image text tuning. In *Proceedings of the IEEE/CVF Conference on Computer Vision and Pattern Recognition*, pages 18123–18133, 2022.
- [4] Lewei Yao, Runhui Huang, Lu Hou, Guansong Lu, Minzhe Niu, Hang Xu, Xiaodan Liang, Zhenguo Li, Xin Jiang, and Chunjing Xu. FILIP: Fine-grained interactive language-image pre-training. In *International Conference on Learning Representations*, 2022.
- [5] Lu Yuan, Dongdong Chen, Yi-Ling Chen, Noel Codella, Xiyang Dai, Jianfeng Gao, Houdong Hu, Xuedong Huang, Boxin Li, Chunyuan Li, et al. Florence: A new foundation model for computer vision. *arXiv preprint arXiv:2111.11432*, 2021.
- [6] Kaiyang Zhou, Jingkang Yang, Chen Change Loy, and Ziwei Liu. Conditional prompt learning for vision-language models. In *Proceedings of the IEEE/CVF Conference on Computer Vision and Pattern Recognition*, pages 16816–16825, 2022.
- [7] Kaiyang Zhou, Jingkang Yang, Chen Change Loy, and Ziwei Liu. Learning to prompt for vision-language models. *International Journal of Computer Vision*, 130(9):2337–2348, 2022.
- [8] Hanoona Abdul Rasheed, Muhammad Maaz, Muhammd Uzair Khattak, Salman Khan, and Fahad Khan. Bridging the gap between object and image-level representations for open-vocabulary detection. In Alice H. Oh, Alekh Agarwal, Danielle Belgrave, and Kyunghyun Cho, editors, *Advances in Neural Information Processing Systems*, 2022.
- [9] Muhammad Maaz, Hanoona Rasheed, Salman Khan, Fahad Shahbaz Khan, Rao Muhammad Anwer, and Ming-Hsuan Yang. Class-agnostic object detection with multi-modal transformer. In *The European Conference on Computer Vision*. Springer, 2022.
- [10] Chengjian Feng, Yujie Zhong, Zequn Jie, Xiangxiang Chu, Haibing Ren, Xiaolin Wei, Weidi Xie, and Lin Ma. Promptdet: Towards open-vocabulary detection using uncurated images. In *European Conference on Computer Vision*, pages 701–717. Springer, 2022.
- [11] Yuhang Zang, Wei Li, Kaiyang Zhou, Chen Huang, and Chen Change Loy. Open-vocabulary detr with conditional matching. *arXiv preprint arXiv:2203.11876*, 2022.
- [12] Boyi Li, Kilian Q Weinberger, Serge Belongie, Vladlen Koltun, and Rene Ranftl. Language-driven semantic segmentation. In *International Conference on Learning Representations*, 2022.

- [13] Yongming Rao, Wenliang Zhao, Guangyi Chen, Yansong Tang, Zheng Zhu, Guan Huang, Jie Zhou, and Jiwen Lu. Denseclip: Language-guided dense prediction with context-aware prompting. In *Proceedings of the IEEE/CVF Conference on Computer Vision and Pattern Recognition*, pages 18082–18091, 2022.
- [14] Jian Ding, Nan Xue, Gui-Song Xia, and Dengxin Dai. Decoupling zero-shot semantic segmentation. In *Proceedings of the IEEE/CVF Conference on Computer Vision and Pattern Recognition*, pages 11583–11592, 2022.
- [15] Timo Lüddecke and Alexander Ecker. Image segmentation using text and image prompts. In *Proceedings of the IEEE/CVF Conference on Computer Vision and Pattern Recognition*, pages 7086–7096, 2022.
- [16] Rui Qian, Yeqing Li, Zheng Xu, Ming-Hsuan Yang, Serge Belongie, and Yin Cui. Multimodal open-vocabulary video classification via pre-trained vision and language models. *arXiv preprint arXiv:2207.07646*, 2022.
- [17] Chen Ju, Tengda Han, Kunhao Zheng, Ya Zhang, and Weidi Xie. Prompting visual-language models for efficient video understanding. In *European Conference on Computer Vision*, pages 105–124. Springer, 2022.
- [18] Timo Schick and Hinrich Schütze. Exploiting cloze questions for few shot text classification and natural language inference. *arXiv preprint arXiv:2001.07676*, 2020.
- [19] Xiang Lisa Li and Percy Liang. Prefix-tuning: Optimizing continuous prompts for generation. *arXiv preprint arXiv:2101.00190*, 2021.
- [20] Brian Lester, Rami Al-Rfou, and Noah Constant. The power of scale for parameter-efficient prompt tuning. *arXiv preprint arXiv:2104.08691*, 2021.
- [21] Xiao Liu, Kaixuan Ji, Yicheng Fu, Zhengxiao Du, Zhilin Yang, and Jie Tang. P-tuning v2: Prompt tuning can be comparable to fine-tuning universally across scales and tasks. *arXiv preprint arXiv:2110.07602*, 2021.
- [22] Taylor Shin, Yasaman Razeghi, Robert L Logan IV, Eric Wallace, and Sameer Singh. Auto-prompt: Eliciting knowledge from language models with automatically generated prompts. In *Proceedings of the 2020 Conference on Empirical Methods in Natural Language Processing (EMNLP)*, pages 4222–4235, 2020.
- [23] Pengfei Liu, Weizhe Yuan, Jinlan Fu, Zhengbao Jiang, Hiroaki Hayashi, and Graham Neubig. Pre-train, prompt, and predict: A systematic survey of prompting methods in natural language processing. *arXiv preprint arXiv:2107.13586*, 2021.
- [24] Zhengbao Jiang, Jun Araki, Haibo Ding, and Graham Neubig. How can we know when language models know? on the calibration of language models for question answering. *Transactions of the Association for Computational Linguistics*, 9:962–977, 2021.
- [25] Menglin Jia, Luming Tang, Bor-Chun Chen, Claire Cardie, Serge Belongie, Bharath Hariharan, and Ser-Nam Lim. Visual prompt tuning. *arXiv preprint arXiv:2203.12119*, 2022.
- [26] Yuanhan Zhang, Kaiyang Zhou, and Ziwei Liu. Neural prompt search. *arXiv preprint arXiv:2206.04673*, 2022.
- [27] Hyojin Bahng, Ali Jahanian, Swami Sankaranarayanan, and Phillip Isola. Visual prompting: Modifying pixel space to adapt pre-trained models. *arXiv preprint arXiv:2203.17274*, 2022.
- [28] Muhammad Uzair Khattak, Hanoona Rasheed, Muhammad Maaz, Salman Khan, and Fahad Shahbaz Khan. Maple: Multi-modal prompt learning. In *Proceedings of the IEEE/CVF Conference on Computer Vision and Pattern Recognition*, pages 19113–19122, 2023.
- [29] Dongjun Lee, Seokwon Song, Jihee Suh, Joonmyeong Choi, Sanghyeok Lee, and Hyunwoo J Kim. Read-only prompt optimization for vision-language few-shot learning. In *Proceedings of the IEEE/CVF International Conference on Computer Vision*, pages 1401–1411, 2023.
- [30] Muhammad Uzair Khattak, Syed Talal Wasim, Muzammal Naseer, Salman Khan, Ming-Hsuan Yang, and Fahad Shahbaz Khan. Self-regulating prompts: Foundational model adaptation without forgetting. In *Proceedings of the IEEE/CVF International Conference on Computer Vision*, pages 15190–15200, 2023.
- [31] Hantao Yao, Rui Zhang, and Changsheng Xu. Visual-language prompt tuning with knowledge-guided context optimization. In *Proceedings of the IEEE/CVF Conference on Computer Vision and Pattern Recognition*, pages 6757–6767, 2023.

- [32] Adrian Bulat and Georgios Tzimiropoulos. Lasp: Text-to-text optimization for language-aware soft prompting of vision & language models. In *Proceedings of the IEEE/CVF Conference on Computer Vision and Pattern Recognition*, pages 23232–23241, 2023.
- [33] Kecheng Zheng, Wei Wu, Ruili Feng, Kai Zhu, Jiawei Liu, Deli Zhao, Zheng-Jun Zha, Wei Chen, and Yujun Shen. Regularized mask tuning: Uncovering hidden knowledge in pre-trained vision-language models. In *Proceedings of the IEEE/CVF International Conference on Computer Vision*, pages 11663–11673, 2023.
- [34] Tianxiang Hao, Xiaohan Ding, Juexiao Feng, Yuhong Yang, Hui Chen, and Guiguang Ding. Quantized prompt for efficient generalization of vision-language models. *arXiv preprint arXiv:2407.10704*, 2024.
- [35] Tianxiang Hao, Hui Chen, Yuchen Guo, and Guiguang Ding. Consolidator: Mergeable adapter with grouped connections for visual adaptation. *arXiv preprint arXiv:2305.00603*, 2023.
- [36] Neil Houlsby, Andrei Giurgiu, Stanislaw Jastrzebski, Bruna Morrone, Quentin De Laroussilhe, Andrea Gesmundo, Mona Attariyan, and Sylvain Gelly. Parameter-efficient transfer learning for nlp. In *International Conference on Machine Learning*, pages 2790–2799. PMLR, 2019.
- [37] Edward J Hu, Yelong Shen, Phillip Wallis, Zeyuan Allen-Zhu, Yuanzhi Li, Shean Wang, Lu Wang, and Weizhu Chen. Lora: Low-rank adaptation of large language models. *arXiv preprint arXiv:2106.09685*, 2021.
- [38] Dongze Lian, Daquan Zhou, Jiashi Feng, and Xinchao Wang. Scaling & shifting your features: A new baseline for efficient model tuning. In *Advances in Neural Information Processing Systems (NeurIPS)*, 2022.
- [39] Shoufa Chen, Chongjian Ge, Zhan Tong, Jiangliu Wang, Yibing Song, Jue Wang, and Ping Luo. Adaptformer: Adapting vision transformers for scalable visual recognition. *Advances in Neural Information Processing Systems*, 35:16664–16678, 2022.
- [40] Xinghao Chen, Yiman Zhang, and Yunhe Wang. Mtp: multi-task pruning for efficient semantic segmentation networks. In *2022 IEEE International Conference on Multimedia and Expo (ICME)*, pages 1–6. IEEE, 2022.
- [41] Ao Wang, Hui Chen, Zijia Lin, Sicheng Zhao, Jungong Han, and Guiguang Ding. Cait: Triple-win compression towards high accuracy, fast inference, and favorable transferability for vits. *arXiv preprint arXiv:2309.15755*, 2023.
- [42] Daniel Bolya, Cheng-Yang Fu, Xiaoliang Dai, Peizhao Zhang, Christoph Feichtenhofer, and Judy Hoffman. Token merging: Your vit but faster. In *The Eleventh International Conference on Learning Representations*, 2023.
- [43] Tianxiang Hao, Xiaohan Ding, Jungong Han, Yuchen Guo, and Guiguang Ding. Manipulating identical filter redundancy for efficient pruning on deep and complicated cnn. *IEEE Transactions on Neural Networks and Learning Systems*, 2023.
- [44] Xiaohan Ding, Tianxiang Hao, Jianchao Tan, Ji Liu, Jungong Han, Yuchen Guo, and Guiguang Ding. Resrep: Lossless cnn pruning via decoupling remembering and forgetting. In *Proceedings of the IEEE/CVF International Conference on Computer Vision*, pages 4510–4520, 2021.
- [45] Xiaohan Ding, Guiguang Ding, Yuchen Guo, and Jungong Han. Centripetal sgd for pruning very deep convolutional networks with complicated structure. In *Proceedings of the IEEE/CVF conference on computer vision and pattern recognition*, pages 4943–4953, 2019.
- [46] Mengzhao Chen, Wenqi Shao, Peng Xu, Mingbao Lin, Kaipeng Zhang, Fei Chao, Rongrong Ji, Yu Qiao, and Ping Luo. Diffrate: Differentiable compression rate for efficient vision transformers. In *Proceedings of the IEEE/CVF International Conference on Computer Vision*, pages 17164–17174, 2023.
- [47] Leqi Shen, Tianxiang Hao, Sicheng Zhao, Yifeng Zhang, Pengzhang Liu, Yongjun Bao, and Guiguang Ding. Tempme: Video temporal token merging for efficient text-video retrieval. *arXiv preprint arXiv:2409.01156*, 2024.
- [48] Yizhe Xiong, Hui Chen, Tianxiang Hao, Zijia Lin, Jungong Han, Yuesong Zhang, Guoxin Wang, Yongjun Bao, and Guiguang Ding. Pyra: Parallel yielding re-activation for training-inference efficient task adaptation. *arXiv preprint arXiv:2403.09192*, 2024.

- [49] Fan Wang, Zhongyi Han, Zhiyan Zhang, Rundong He, and Yilong Yin. Mhpl: Minimum happy points learning for active source free domain adaptation. In *Proceedings of the IEEE/CVF Conference on Computer Vision and Pattern Recognition*, pages 20008–20018, 2023.
- [50] Mengyao Lyu, Tianxiang Hao, Xinhao Xu, Hui Chen, Jungong Han, and Guiguang Ding. Learn from the learnt: Source-free active domain adaptation via contrastive sampling and visual persistence. In *European Conference on Computer Vision (ECCV)*. Springer, 2024.
- [51] Alexey Dosovitskiy, Lucas Beyer, Alexander Kolesnikov, Dirk Weissenborn, Xiaohua Zhai, Thomas Unterthiner, Mostafa Dehghani, Matthias Minderer, Georg Heigold, Sylvain Gelly, et al. An image is worth 16x16 words: Transformers for image recognition at scale. In *International Conference on Learning Representations*, 2020.
- [52] Beier Zhu, Yulei Niu, Yucheng Han, Yue Wu, and Hanwang Zhang. Prompt-aligned gradient for prompt tuning. In *Proceedings of the IEEE/CVF International Conference on Computer Vision*, pages 15659–15669, 2023.
- [53] Jianxiong Xiao, James Hays, Krista A Ehinger, Aude Oliva, and Antonio Torralba. Sun database: Large-scale scene recognition from abbey to zoo. In *CVPR*, 2010.
- [54] Mircea Cimpoi, Subhransu Maji, Iasonas Kokkinos, Sammy Mohamed, and Andrea Vedaldi. Describing textures in the wild. In *CVPR*, 2014.
- [55] Yongqin Xian, Bernt Schiele, and Zeynep Akata. Zero-shot learning-the good, the bad and the ugly. In *CVPR*, 2017.
- [56] Peng Gao, Shijie Geng, Renrui Zhang, Teli Ma, Rongyao Fang, Yongfeng Zhang, Hongsheng Li, and Yu Qiao. Clip-adapter: Better vision-language models with feature adapters. *arXiv preprint arXiv:2110.04544*, 2021.
- [57] Kaiming He, Xiangyu Zhang, Shaoqing Ren, and Jian Sun. Deep residual learning for image recognition. In *Proceedings of the IEEE conference on computer vision and pattern recognition*, pages 770–778, 2016.
- [58] Jia Deng, Wei Dong, Richard Socher, Li-Jia Li, Kai Li, and Li Fei-Fei. Imagenet: A large-scale hierarchical image database. In *CVPR*, 2009.
- [59] Li Fei-Fei, Rob Fergus, and Pietro Perona. Learning generative visual models from few training examples: An incremental bayesian approach tested on 101 object categories. In *CVPR-W*, 2004.
- [60] Omkar M Parkhi, Andrea Vedaldi, Andrew Zisserman, and CV Jawahar. Cats and dogs. In *CVPR*, 2012.
- [61] Jonathan Krause, Michael Stark, Jia Deng, and Li Fei-Fei. 3d object representations for fine-grained categorization. In *ICCV-W*, 2013.
- [62] Maria-Elena Nilsback and Andrew Zisserman. Automated flower classification over a large number of classes. In *ICVGIP*, 2008.
- [63] Lukas Bossard, Matthieu Guillaumin, and Luc Van Gool. Food-101—mining discriminative components with random forests. In *ECCV*, 2014.
- [64] Subhransu Maji, Esa Rahtu, Juho Kannala, Matthew Blaschko, and Andrea Vedaldi. Fine-grained visual classification of aircraft. *arXiv preprint arXiv:1306.5151*, 2013.
- [65] Khurram Soomro, Amir Roshan Zamir, and Mubarak Shah. Ucf101: A dataset of 101 human actions classes from videos in the wild. *arXiv preprint arXiv:1212.0402*, 2012.
- [66] Patrick Helber, Benjamin Bischke, Andreas Dengel, and Damian Borth. Eurosat: A novel dataset and deep learning benchmark for land use and land cover classification. *IEEE Journal of Selected Topics in Applied Earth Observations and Remote Sensing*, 2019.
- [67] Dan Hendrycks, Kevin Zhao, Steven Basart, Jacob Steinhardt, and Dawn Song. Natural adversarial examples. *CVPR*, 2021.
- [68] Dan Hendrycks, Steven Basart, Norman Mu, Saurav Kadavath, Frank Wang, Evan Dorundo, Rahul Desai, Tyler Zhu, Samyak Parajuli, Mike Guo, Dawn Song, Jacob Steinhardt, and Justin Gilmer. The many faces of robustness: A critical analysis of out-of-distribution generalization. *ICCV*, 2021.

- [69] Benjamin Recht, Rebecca Roelofs, Ludwig Schmidt, and Vaishaal Shankar. Do imagenet classifiers generalize to imagenet? In *International conference on machine learning*, pages 5389–5400. PMLR, 2019.
- [70] Haohan Wang, Songwei Ge, Zachary Lipton, and Eric P Xing. Learning robust global representations by penalizing local predictive power. In *Advances in Neural Information Processing Systems*, pages 10506–10518, 2019.
- [71] Norman Mu, Alexander Kirillov, David Wagner, and Saining Xie. Slip: Self-supervision meets language-image pre-training. In *European conference on computer vision*, pages 529–544. Springer, 2022.

A Datasets

Following previous work [7, 6], we leverage 11 image recognition datasets to verify the effectiveness of the proposed method for both the base-to-new generalization task. These datasets include two datasets for the generic object classification, *i.e.*, ImageNet [58] and Caltech101 [59], five datasets for the fine-grained classification, *i.e.*, OxfordPets [60], StanfordCars [61], Flowers102 [62], Food101 [63] and FGVC Aircraft [64], one dataset for the scene recognition, *i.e.*, SUN397 [53], one dataset for the action recognition, *i.e.*, UCF101 [65], one dataset for the texture classification, *i.e.*, DTD [54], and one dataset for the satellite imagery recognition, *i.e.*, EuroSAT [66]. Following previous works [6, 7], for each dataset, we split its classes equally into two non-overlapping groups, *i.e.*, one as base classes and the other as new classes. We train all models on the base classes and perform a base/new evaluation on the base/new classes.

For the domain generalization task, we utilize ImageNet-A [67], ImageNet-R [68], ImageNetv2 [69] and ImageNet-S [70] to verify the robustness of the model. In this setting, we need to first train the model using ImageNet, and then directly use images from other four datasets to do inference.

For the cross-dataset transfer task, the datasets are the same as those of the base-to-new generalization task. Similar to domain generalization, the model will be first trained on ImageNet and then do inference on the other 10 different datasets.

For the few-shot learning task, the datasets are the same as those of the base-to-new generalization task. The model will be trained and evaluated with 1, 2, 4, 8 and 16 shots separately.

The dataset splitting is exactly the same as previous works [7, 6]. We report the averaged model performance over three runs with different random seeds for fair comparisons.

B Training Details

Following previous work [6], we employ ViT-B/16 as the image encoder in the CLIP. Each training image is resized to 224×224 before being fed into the image encoder. Some common data augmentation strategies, *e.g.*, random crop and random flip, are used to enhance the model performance, following [6]. During training, we set the batch size as 32. We employ the stochastic gradient descent algorithm (SGD) to optimize the learnable parameters. As [7], we utilize a warm-up scheme at the first epoch, which is important for the tuning of prompts. For all the other baselines, we strictly follow the configurations of their original papers.

To verify the effectiveness of our proposed method, we explore the improvement of integrating DIP into a lightweight prompt tuning method CoOp and a heavy prompt tuning method MaPLe separately.

For DIP+CoOp and DIP+MaPLe, we conduct a grid search to find the optimal hyper-parameters based on the configuration of CoOp and MaPLe. In the main text, we set the rank $r = 1$ in DIP for all the experiments unless specially mentioned. The total number of tunable parameters in DIP+CoOp is $4 * 1 + 1 * 512 = 516$, which is merely around 0.25x of that in CoOp. For DIP+MaPLe, we also decompose its weights of the projection layer that projects text prompts to generate image prompts with rank $r_{proj} = 64$. Therefore, the total number of tunable parameters in DIP+MaPLe is $(4 * 1 + 1 * 512) + (512 * 64 + 64 * 768) = 82436$ per layer, and $82436 * 9 = 741924$ in total for 9 layers are modified in MaPLe by default.

Table 9: Detailed comparisons with latest methods in base-to-new generalization. H: harmonic mean [55]. DIP+CoOp outperforms all the other lightweight methods on 8 out of 11 datasets, and DIP+MaPLe achieves better harmonic mean accuracy on 9 out of 11 datasets compared to MaPLe alone. Better still, methods modified by DIP even enjoys significantly better parameter efficiency.

(a) Parameters comparison.

| Method | CoOp | CoCoOp | Adapter | LoRA | ProGrad | DIP+CoOp | MaPLe | DIP+MaPLe |
|---------|------|--------|---------|--------|---------|----------|-------|-----------|
| #params | 2.1K | 35.4K | 525.5K | 129.0K | 8.2K | 0.5K | 3548K | 741.9K |

(b) Average.

| | Base | New | H |
|-----------|-------|-------|-------|
| CLIP | 69.34 | 74.22 | 71.70 |
| CoOp | 82.69 | 63.22 | 71.66 |
| CoCoOp | 80.47 | 71.69 | 75.83 |
| Adapter | 82.62 | 70.97 | 76.35 |
| LoRA | 84.30 | 67.33 | 74.86 |
| ProGrad | 82.79 | 68.55 | 75.00 |
| DIP+CoOp | 80.32 | 74.73 | 77.42 |
| MaPLe | 82.28 | 75.14 | 78.55 |
| DIP+MaPLe | 83.17 | 75.43 | 79.11 |

(c) ImageNet.

| | Base | New | H |
|-----------|-------|-------|-------|
| CLIP | 72.43 | 68.14 | 70.22 |
| CoOp | 76.47 | 67.88 | 71.92 |
| CoCoOp | 75.98 | 70.43 | 73.10 |
| Adapter | 76.53 | 66.67 | 71.26 |
| LoRA | 74.77 | 58.47 | 65.62 |
| ProGrad | 77.03 | 68.80 | 72.68 |
| DIP+CoOp | 76.10 | 71.17 | 73.55 |
| MaPLe | 76.66 | 70.54 | 73.47 |
| DIP+MaPLe | 76.80 | 70.97 | 73.77 |

(d) Caltech101.

| | Base | New | H |
|-----------|-------|-------|-------|
| CLIP | 96.84 | 94.00 | 95.40 |
| CoOp | 98.00 | 89.81 | 93.73 |
| CoCoOp | 97.96 | 93.81 | 95.84 |
| Adapter | 98.20 | 93.20 | 95.63 |
| LoRA | 98.49 | 90.33 | 94.24 |
| ProGrad | 98.50 | 91.90 | 95.09 |
| DIP+CoOp | 98.10 | 95.23 | 96.65 |
| MaPLe | 97.74 | 94.36 | 96.02 |
| DIP+MaPLe | 98.20 | 94.83 | 96.49 |

(e) OxfordPets.

| | Base | New | H |
|-----------|-------|-------|-------|
| CLIP | 91.17 | 97.26 | 94.12 |
| CoOp | 93.67 | 95.29 | 94.47 |
| CoCoOp | 95.20 | 97.69 | 96.43 |
| Adapter | 94.40 | 94.10 | 94.25 |
| LoRA | 94.90 | 92.57 | 93.72 |
| ProGrad | 94.40 | 95.10 | 94.75 |
| DIP+CoOp | 95.53 | 97.93 | 96.72 |
| MaPLe | 95.43 | 97.76 | 96.58 |
| DIP+MaPLe | 95.67 | 98.00 | 96.82 |

(f) StanfordCars.

| | Base | New | H |
|-----------|-------|-------|-------|
| CLIP | 63.37 | 74.89 | 68.65 |
| CoOp | 78.12 | 60.40 | 68.13 |
| CoCoOp | 70.49 | 73.59 | 72.01 |
| Adapter | 77.13 | 69.23 | 72.97 |
| LoRA | 81.07 | 65.30 | 72.34 |
| ProGrad | 79.00 | 67.93 | 73.05 |
| DIP+CoOp | 71.33 | 74.47 | 72.87 |
| MaPLe | 72.94 | 74.00 | 73.47 |
| DIP+MaPLe | 76.00 | 73.00 | 74.47 |

(g) Flowers102.

| | Base | New | H |
|-----------|-------|-------|-------|
| CLIP | 72.08 | 77.80 | 74.83 |
| CoOp | 97.60 | 59.67 | 74.06 |
| CoCoOp | 94.87 | 71.75 | 81.71 |
| Adapter | 97.70 | 70.83 | 82.13 |
| LoRA | 98.23 | 60.20 | 74.65 |
| ProGrad | 96.27 | 71.07 | 81.77 |
| DIP+CoOp | 95.53 | 75.23 | 84.18 |
| MaPLe | 95.92 | 72.46 | 82.56 |
| DIP+MaPLe | 97.00 | 73.77 | 83.80 |

(h) Food101.

| | Base | New | H |
|-----------|-------|-------|-------|
| CLIP | 90.10 | 91.22 | 90.66 |
| CoOp | 88.33 | 82.26 | 85.19 |
| CoCoOp | 90.70 | 91.29 | 90.99 |
| Adapter | 90.40 | 90.40 | 90.40 |
| LoRA | 88.57 | 87.30 | 87.93 |
| ProGrad | 90.17 | 89.53 | 89.85 |
| DIP+CoOp | 90.83 | 92.03 | 91.43 |
| MaPLe | 90.71 | 92.05 | 91.38 |
| DIP+MaPLe | 90.63 | 91.90 | 91.26 |

(i) FGVCaircraft.

| | Base | New | H |
|-----------|-------|-------|-------|
| CLIP | 27.19 | 36.29 | 31.09 |
| CoOp | 40.44 | 22.30 | 28.75 |
| CoCoOp | 33.41 | 23.71 | 27.74 |
| Adapter | 39.57 | 32.27 | 35.55 |
| LoRA | 46.27 | 28.83 | 35.53 |
| ProGrad | 42.63 | 26.97 | 33.04 |
| DIP+CoOp | 35.17 | 35.57 | 35.37 |
| MaPLe | 37.44 | 35.61 | 36.50 |
| DIP+MaPLe | 39.03 | 37.17 | 38.08 |

(j) SUN397.

| | Base | New | H |
|-----------|-------|-------|-------|
| CLIP | 69.36 | 75.35 | 72.23 |
| CoOp | 80.60 | 65.89 | 72.51 |
| CoCoOp | 79.74 | 76.86 | 78.27 |
| Adapter | 81.67 | 73.93 | 77.61 |
| LoRA | 79.73 | 69.00 | 73.98 |
| ProGrad | 80.70 | 71.03 | 75.56 |
| DIP+CoOp | 79.60 | 77.80 | 78.69 |
| MaPLe | 80.82 | 78.70 | 79.75 |
| DIP+MaPLe | 81.27 | 78.13 | 79.67 |

(k) DTD.

| | Base | New | H |
|-----------|-------|-------|-------|
| CLIP | 53.24 | 59.90 | 56.37 |
| CoOp | 79.44 | 41.18 | 54.24 |
| CoCoOp | 77.01 | 56.00 | 64.85 |
| Adapter | 80.47 | 52.23 | 63.35 |
| LoRA | 82.93 | 54.90 | 66.06 |
| ProGrad | 76.70 | 46.67 | 58.03 |
| DIP+CoOp | 75.67 | 60.43 | 67.20 |
| MaPLe | 80.36 | 59.18 | 68.16 |
| DIP+MaPLe | 82.10 | 59.50 | 69.00 |

(l) EuroSAT.

| | Base | New | H |
|-----------|-------|-------|-------|
| CLIP | 56.48 | 64.05 | 60.03 |
| CoOp | 92.19 | 54.74 | 68.69 |
| CoCoOp | 87.49 | 60.04 | 71.21 |
| Adapter | 86.93 | 64.20 | 73.86 |
| LoRA | 94.90 | 65.67 | 77.62 |
| ProGrad | 91.37 | 56.53 | 69.85 |
| DIP+CoOp | 82.70 | 65.40 | 73.04 |
| MaPLe | 94.07 | 73.23 | 82.35 |
| DIP+MaPLe | 93.67 | 74.33 | 82.89 |

(m) UCF101.

| | Base | New | H |
|-----------|-------|-------|-------|
| CLIP | 70.53 | 77.50 | 73.85 |
| CoOp | 84.69 | 56.05 | 67.46 |
| CoCoOp | 82.33 | 73.45 | 77.64 |
| Adapter | 85.80 | 73.63 | 79.25 |
| LoRA | 87.47 | 68.03 | 76.53 |
| ProGrad | 83.90 | 68.50 | 75.42 |
| DIP+CoOp | 82.93 | 76.70 | 79.69 |
| MaPLe | 83.00 | 78.66 | 80.77 |
| DIP+MaPLe | 84.50 | 78.13 | 81.19 |

Table 10: Base-to-new generaliation performances based on SLIP [71].

| | #params | base | new | H |
|----------|---------|--------------|--------------|--------------|
| CoOp | 2.1K | 68.45 | 42.77 | 52.64 |
| DIP+CoOp | 0.5K | 62.53 | 47.78 | 54.17 |

Table 11: Results of different combinations of learning rates and weight decays under 16-shot learning setting on ImageNet

| Acc | wd | lr | | |
|------|----|-------|-------|-------|
| | | 1e-4 | 5e-4 | 1e-3 |
| 1e-3 | | 70.73 | 70.67 | 70.78 |
| 2e-3 | | 70.80 | 70.83 | 70.77 |
| 3e-3 | | 70.83 | 70.83 | 70.81 |

C Competitors

1. **CLIP** [1]: CLIP is a strong baseline vision-language model that is pre-trained on a large number of image-text pairs from the web by learning a contrastive objective. CLIP enables strong zero-shot adaptation ability on various downstream tasks by using fixed text prompts, *i.e.* *a photo of a*.
2. **CoOp** [7]: CoOp replaces the fixed text prompts in CLIP with tunable text prompts to improve the adaptation ability of the vision-language model. CoOp shows excellent performance in few-shot situations.
3. **CoCoOp** [6]: CoCoOp replaces the isolated tunable text prompts in CoOp with conditional text prompts, which receive extra gradients from the image features besides text features. CoCoOp largely improves the generalization ability of the vision-language model, getting good results on base-to-new generalization and domain adaptation.
4. **CLIP-Adapter** [56]: CLIP-Adapter adopts the thoughts of classic Adapter [36] to use serial linear layers and activation functions to adapt for downstream tasks. It is simple yet effective in few-shot learning.
5. **LoRA** [37]: LoRA adopts low-rank decomposition for weights in FC layers. It is efficient and earns good results in NLP field.
6. **MaPLe** [28]: MaPLe simultaneously adds prompts to the image encoder and text encoder of CLIP. To trigger more information exchange between the image side and text side, MaPLe generate image prompts from the projection of text prompts. Though effective, such design brings quite heavy cost.
7. **ProGrad** [52]: ProGrad only updates the text and image prompts whose gradient are aligned (or non-conflicting) to the general knowledge, which is represented as the optimization direction offered by the pre-defined prompt predictions. Such regularization helps it finish good adaptation and generalization.

D Complete Results in Base-To-New Generalization

As shown in Tab. 9, overall, DIP shows quite competitive performance, and the superiority mainly relies on the improvement of new class accuracy. In other words, DIP largely improves the generalization ability of CLIP. In particular, compared with CoOp, DIP+CoOp gets 10.95% accuracy gain

Table 12: Deep prompts in different depths for DIP+CoOp.

| depth | #params | base | new | H |
|-------|---------|-------|-------|-------|
| 1 | 0.5K | 76.37 | 74.69 | 75.52 |
| 2 | 1.0K | 77.81 | 73.87 | 75.79 |
| 3 | 1.5K | 79.55 | 72.72 | 75.98 |
| 4 | 2.0K | 80.07 | 72.69 | 76.20 |
| 5 | 2.6K | 80.24 | 73.37 | 76.65 |
| 6 | 3.1K | 80.64 | 73.39 | 76.85 |

Table 13: Training, storage, and inference efficiencies.

| | #params | Training throughput | Inference throughput |
|----------|-------------|---------------------|----------------------|
| CoOp | 2.1K | 93 image/s | 738 images/s |
| CoCoOp | 35.4K | 5 images/s | 13 images/s |
| ProGrad | 8.2K | 56 images/s | 732 images/s |
| DIP+CoOp | 0.5K | 91 images/s | 738 images/s |

on the new classes and 2.83% accuracy drop on the base classes, showing strongest harmonic mean accuracy on 8 out of 11 datasets among all the lightweight existing methods. Compared with a heavy method MaPLe, DIP+MaPLe achieves better harmonic mean accuracy on 9 out of 11 datasets.

E Experiments on a Different Vision-Language Architecture

In this paragraph, we show the results of DIP on another vision-language architecture, SLIP [71], besides CLIP. Seen from Tab. 10, DIP+CoOp earns much higher new accuracy and harmonic mean accuracy than the original CoOp.

F Effect of Deep Prompts

In this paragraph, we extend the shallow prompts in DIP+CoOp to the deep prompts. We record the accuracy change as we increase the layers including tunable prompts, following the last equation in Section 3.1 in the main text. Results are shown in Tab. 12. As the depth increases, the base accuracy keeps increasing while the new accuracy first decreases and then increases. Overall, more depth generally leads to higher harmonic mean accuracy. Therefore, it is possible to further improve the performance of our method by increasing the prompt depth.

G Effect of Different learning rates and Weight Decays

In this paragraph, we investigate the effect of normal hyper-parameters learning rate and weight decay. We wonder if tuning them carefully would lead to significant improvement. Seen from Tab. 11, the performance of DIP stays stable whatever the learning rate and weight decay vary. The conclusion here is that our method DIP is robust for learning rate and weight decay.

H Efficiency Comparison

In this paragraph, we will give a comprehensive analysis of all the training, storage, and inference efficiencies for DIP and several existing methods. Since the parameter scale of CLIP-Adapter [56] is significantly larger than others, we do not contain CLIP-Adapter into comparison.

For a fair comparison, we do all the speed tests on the same GPU. Results are shown in Tab. 13. Our proposed DIP shares nearly the same fastest training and inference speeds with the simplest method CoOp, and more importantly, DIP merely uses 0.5K parameters, which is a lot more storage-efficient than other methods. Specially, compared with classic method CoCoOp, DIP enjoys **>18x** training speed, **>56x** inference speed and **<70x** storage usage. Besides complex structures, the huge gap in the inference speed is partly owing to the huge memory cost of CoCoOp, which forces us to adopt a smaller batch size than other methods for CoCoOp. Moreover, compared with the latest method ProGrad, DIP enjoys **>1.6x** training speed, comparable inference speed, and **<60x** storage usage, which adequately demonstrates the super efficiency of DIP.